Short-Fluorinated iCVD Coatings for Nonwetting Fabrics

DOI: 10.1002/((please add manuscript number))

Article type: Communication

Short-fluorinated iCVD coatings for non-wetting fabrics

*Dan Soto, Asli Ugur, Taylor A. Farnham, Karen K. Gleason and Kripa K. Varanasi**

Dr. D. Soto, T. A. Farnham and Prof. K. K. Varanasi

Department of Mechanical Engineering, Massachusetts Institute of Technology, Cambridge, MA 02139, USA.

EMail: varanasi@mit.edu

Dr. A. Ugur and Prof. K. K. Gleason

Department of Chemical Engineering, Massachusetts Institute of Technology, Cambridge, Massachusetts 02139, USA.

EMail: kkgleasn@mit.edu

Keywords: Short-fluorinated polymer; initiated Chemical Vapor Deposition (iCVD); hydrophobic coating; micro-sandblasting; fabrics and textiles

Water repellency is most often generated by taking advantage of surface textures[1,2] and low surface energy coatings such as the one afforded by polymers possessing long perfluorinated side chains [3–

[6]. However, perfluorinated chains of eight carbons or more, have been shown to be persistent in the environment and bio-accumulate in living organisms[7]. Because of the related health and safety hazard concerns, governmental agencies are phasing out and banning these polymers, requiring the search for, and use of, new chemistries with shorter perfluorinated side chains[8]. This is a particular challenge for water-repellent fabrics as textile coatings are commonly applied via liquid phase processes[9] which requires forcing the liquid into the pores, drying them without clogging and taking care of waste management. Hence, in the midst of the textile technological evolution embodied by the development of the so called 'smart fabrics', initiated chemical vapor deposition[10] (iCVD) appears as a new promising technique; iCVD allows the deposition of ultra-thin conformal durable and breathable coatings and paves the path to new types of functionalization such as charge management capabilities[11].

In this work, we develop an approach that allows for iCVD deposition of conformal short fluorinated polymers stabilized with a crosslinking agent and report the successful iCVD polymerization of 1*H*,1*H*-Perfluorooctyl methacrylate crosslinked with divinylbenzene. We explain why this coating having less than eight perfluorinated sidechain carbons exhibit remarkable hydrophobic properties and low adhesion amidst a wide range of other possible candidates making it a suitable candidate to replace the more persistent polymers that are being banned. In order to further enhance the dynamic water repellency performance, we combine the chemical treatment with physical texturing done through micro-sandblasting, a process particularly suitable for fabrics. Finally, we show how the iCVD growth method results in durable and breathable coatings and allows to extend the range of applications to substrates as diverse as fabrics, paper, and nano-textured silicon.

The iCVD process is a single-step vapor-phase method used to deposit conformal polymer films with a controllable thickness[10] and texture[10,12,13]. In addition, the potential to graft the polymer directly to the substrate enhances coating durability[14,15]. The side chains of these polymer films, grown through radical polymerization[10], play a key role in the macroscopic properties of the films. Indeed, it has been shown that the highest hydrophobicity, that is, the lowest surface energy, is chemically achieved with $-CF_3$ groups (followed by $-CF_2H$, $-CF_2$, $-CH_3$, $-CH_2$, respectively in terms of decreasing hydrophobicity). In that perspective, side chains can be seen as fluorine carriers site (see **Figure 1a**) that lead to surface energies as low as 6 mN m^{-1} when uniformly structured[16]. Since such low surface energies - giving rise to extremely non-wetting substrates - can only be achieved with fluorinated chemistries, traditional and widely used silicon based coatings do not provide suitable replacement solutions[17]. Because side chains can reorient upon interaction with different media[18] they can lead to increased contact angle hysteresis (CAH) and pinning. Hence, it is important to control fluorine content and minimize pendant chains reorientation ability. Up to now, long side chain fluorinated polymers have been widely used because of their ability to crystalize[16,19–21] , yielding outstanding performances in terms of water repellency, CAH[22] and stability. However, another consequence of

this crystallization is their difficulty to be degraded, which leads to their bioaccumulation and potential environmental and health risks and makes them unsuitable for most applications.

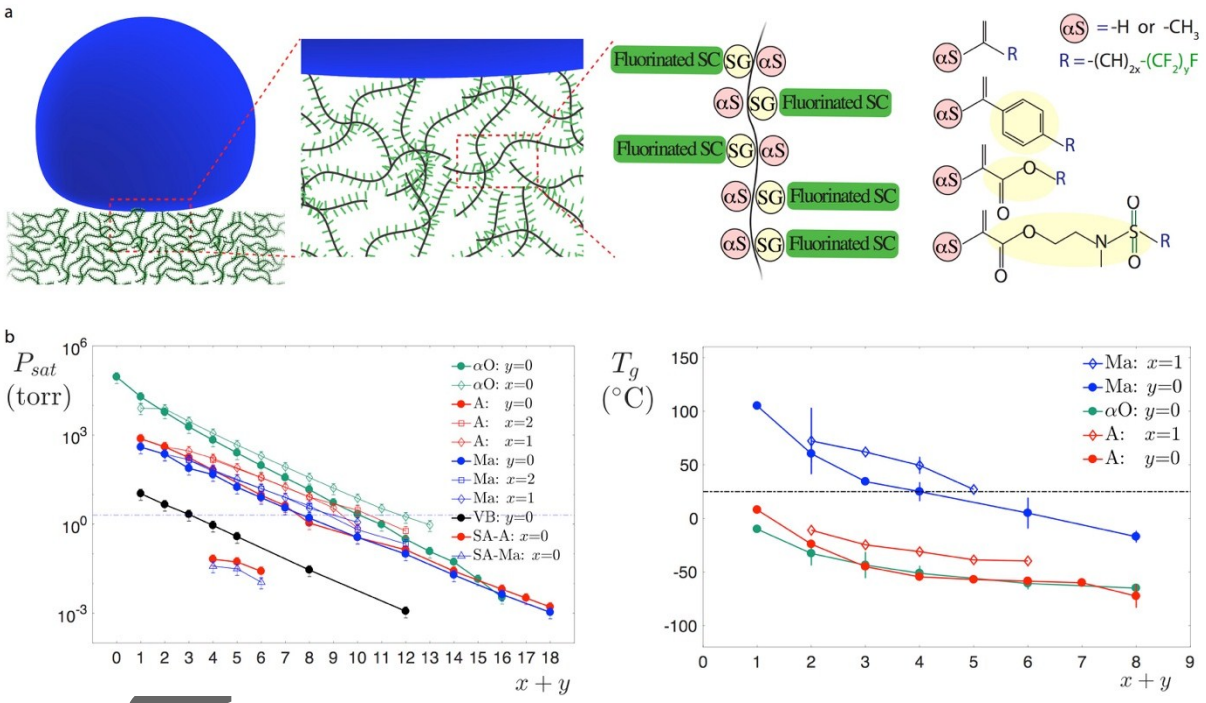

Figure 1. a) Schematic view of coating where side chains consisting of a tail can carry the fluorinated groups (Fluorinated SC, solid green) and are attached to the backbone through a Spacer Group (SG, shaded yellow). A bulky alpha-Substituent (αS, shaded red) will limit side chain mobility. Right panel: monomers suitable for free radical polymerization: olefin, vinylbenzene derivates, (Meth)-acrylate and Sulfonamide (Meth)-acrylate. The end of the side chain (*R*-) has *x* hydrogenated and *y* fluorinated carbons. b) and c) Monomer vapor pressure (at 80 °C) and glass transition temperature T_g as a function of side chain length *x+y*: in green, olefins (αO); in red, acrylates (A) and sulfonamide acrylate (SA-A); in blue, methacrylates (MA) and sulfonamide methacrylate (SA-M); in black, vinyl benzene (VB). Data from literature values as described in SI.

Recent reports explore hydrophobic short-fluorinated solutions [16,23–25] that draw their performances from the crystallization of heavy-molecule monomers. However, due to their low volatility, they cannot be vapor deposited and face all limitations of liquid-based solutions, among which the challenge of forcing the liquid coating into the roughness or pores of the textiles – a major obstacle to coat ever smaller features. For vapor deposition approaches, the consequences of going to short-fluorinated side chain polymers (fewer than 8 perfluorinated carbons) are hence drastic: the polymer will not crystallize anymore and its amorphous nature (T_g decreasing with increasing side chain length[26], see **Figure 1c**) will lead to increased side chain mobility. Considering that fluorine content needs to be kept as high as possible in order to have low surface energies and high contact angles, we need to identify the best vaporizable monomer candidate with 7 fluorinated carbons (see **Figure 1c** and supplementary information) and optimize its side chain interactions by tuning the main

chain flexibility[27], the stiffness of the spacer group[25], and the geometrical hindering of substituents[24]. The fluorinated tails can be attached to a wide range of reactive heads allowing us to select the ones which are most suitable for radical chain polymerization process[28]: olefins, vinylbenzenes, acrylates, methacrylates, and their derivatives (see **Figure 1a**, forth panel). Among these options, only the monomers that are able to evaporate into the reactor chamber can be used with iCVD process (typical vapor pressure above 1 Torr). We observe in **Figure 1b** that although the vinylbenzene derivate (VB), the sulfonamide acrylates (SA-A) and sulfonamide methacrylates[16,25] (SAMa) are good candidates – they have a stiff and bulky spacer group preventing chain mobility – they are too heavy to be easily vaporized. Finally, we expect that stiffer spacer group (only one -CH_2- group between the head and the fluorinated chain being the stiffest solution) as well as a bulky alpha substituent[24] will reduce side chain mobility, suggesting 1*H*,1*H*-perfluorooctyl methacrylate (H_1F_7Ma) as the best candidate. Indeed, this lack of mobility can be also observed in **Figure 1c** where for a given side chain length, the highest T_g corresponds to the case of methacrylates.

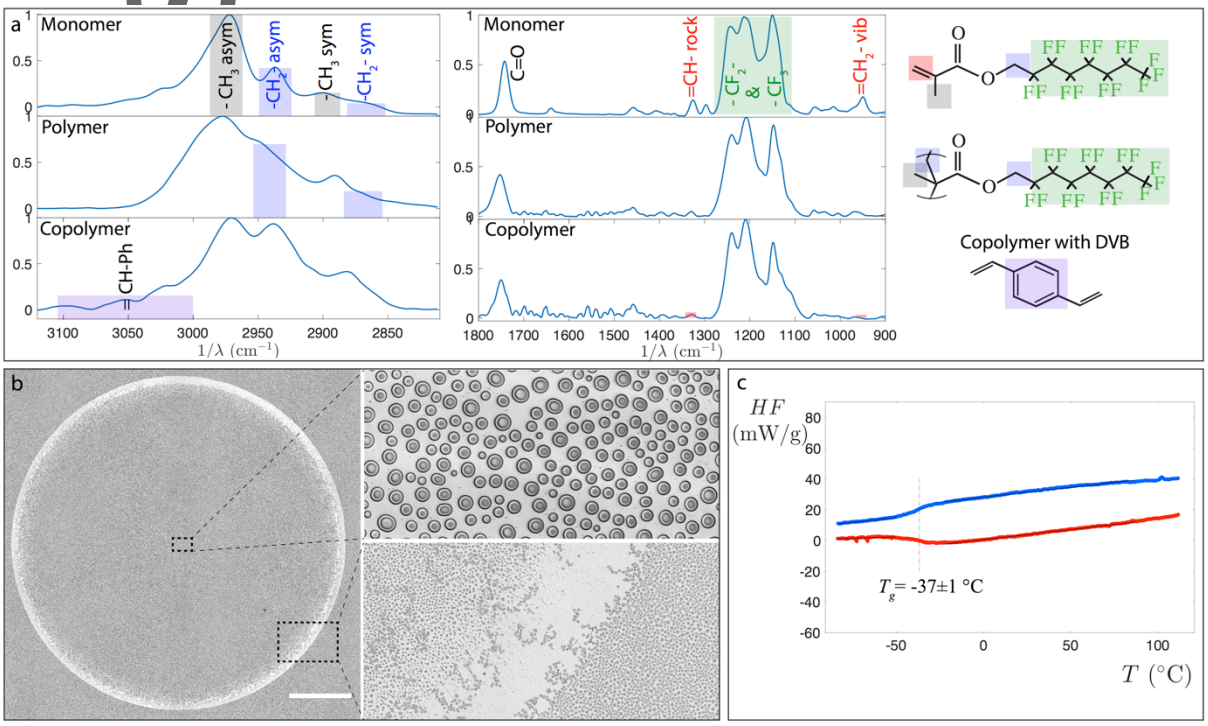

Figure 2. a) FTIR spectra of H_1F_7Ma monomer (top row), H_1F_7Ma homopolymer (middle row) and H_1F_7Ma-co-DVB copolymer (bottom row, 34% DVB content). Spectra were normalized by the -CH_3 and CF_2 & CF_3 peaks for the 2800-3100 cm^{-1} and 900-1800 cm^{-1} region respectively. On the right, shaded areas correspond to functional groups highlighted in the FTIR spectra. b) Microscopic top view of a mark left on homopolymer coating on a flat silicon substrate after water droplet removal. Scale bar: 0.5 mm. Close-up views correspond to selected regions: top one shows destabilization of the coating into droplets; bottom one shows coating droplets displaced at the triple contact line after drop removal. c) Heat flux (mW/g) of H_1F_7Ma homopolymer as a function of temperature showing a glass transition temperature T_g = -37 °C.

In order to deposit H_1F_7Ma via iCVD, the monomer is heated at 80 °C and the vapor phase is introduced into a reactor chamber at several hundred millitorr. The gaseous initiator tert-butyl

peroxide (TBPO) is activated via heating filaments and polymerization of a film of typical thickness 100 nm (see Table S1) is enabled directly onto the surface of a flat (silicon substrate) or textured (fabric) substrate (see detailed deposition conditions in SI). To ensure the successful polymerization of the new monomer, in **Figure 2a**, we compare its FTIR spectra to the polymer. Normalizing the region 2850-3000 cm^{-1} by the total intensity of the $-CH_3$ asymmetric vibration peak (grey region at 2975 cm^{-1}, expected to remain unchanged through polymerization) we can observe a relative increase of the $-CH_2-$ asymmetric peak (blue region at 2940 cm^{-1}) for the polymer case, confirming the formation of a backbone chain. Similarly, normalizing the region 900-1400 cm^{-1} by the intensity of the bands attributed to the $-CF_2-$, $-CF_3$ moieties (green region at 1146 and 1240 cm^{-1} respectively, expected also to remain unchanged), we observe a relative decrease of the =CH- rocking and $=CH_2$ vibrational peaks (red regions at 1327 and 950 cm^{-1}, respectively), confirming the successful formation of the expected polymer. Although the coating deposited onto a flat silicon surface shows a very good advancing contact angle (close to the theoretical limit of 120 degrees, see **Figure 3a**) the receding contact angle is extremely low and the water droplet exhibits considerable pinning. Indeed, when removing the drop, a visible mark is left behind (see **Figure 2b** and **Movie 1**), an indication that the coating is not stable. Microscope examination after polymerization shows that the film has destabilized into tiny droplets[29,30] that can be displaced by the water at the contact line[31], creating this unusual highly pinning behavior. To further understand this behavior, the glass transition temperature T_g for the homopolymer is measured with differential scanning calorimetry (DSC) and found to be around -37 °C (see **Figure 2c**), in agreement with trends shown in **Figure 1c** and confirming that the coating was an elastomer allowing the film to destabilize.

To overcome this limitation we crosslink H_1F_7Ma with DVB[14,15] and verify the presence of the crosslinker in the copolymer by the appearance of band around 3050 cm^{-1} (a signature of the benzene =CH bond, see **Figure 2a**) in the FTIR spectra. Indeed, when measuring the dynamic contact angle of water across copolymer coatings with different DVB content (**Figure 3a**, from 10% to 60% DVB) we observe that the film is now stabilized and retains the high hydrophobicity of the fluorinated H_1F_7Ma homopolymer as well as the low CAH of pure DVB.

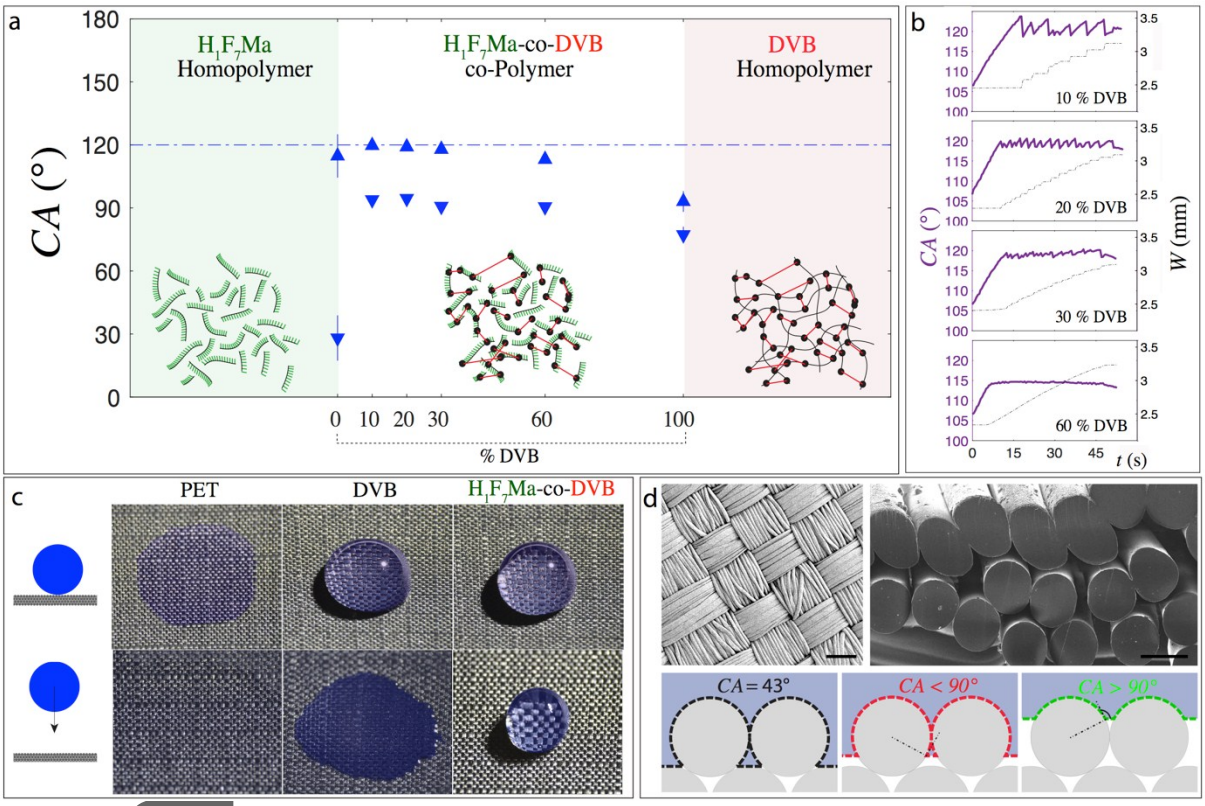

Figure 3. a) Advancing and receding contact angle (upward and downward triangle respectively) for water measured on flat silicon substrate coated with different H_1F_7Ma and DVB contents. Sketch shows how DVB acts as a crosslinker by building bridges between backbones of different polymer chains. The dashed horizontal line marks the theoretical limit of 120°. b) Contact angle (left axis) and width *W* of contact area of droplet (right axis) for a droplet placed on a flat substrate coated with different DVB content and whose volume is gradually increasing from 5 µL to 15 µL. c) Typical droplet outcome after being deposited (top row) or impacted (bottom row) against a polyester fabric left untreated (left), coated with DVB (middle) and coated with H_1F_7Ma-co-DVB (60% DVB, right). The wetted area has been colored with blue for increased clarity. d) SEM top view (left, scale represents 100 µm) and cross section (right, scale represents 10 µm) of a typical outdoor garment fabric. Impregnation model across stacked cylinders (bottom sketch): the more hydrophobic the chemistry, the more robust will be the fabric regarding water penetration.

In order to find the optimal composition of the film we show in **Figure 3b** the temporal behavior of the advancing contact angle for the different DVB compositions. Below 30% DVB content, a "stick–slip" behavior can be observed due to the low crosslinking rate of DVB leading to increased CAH. Above 60% DVB, this phenomenon is suppressed but the overall hydrophobicity starts to decrease because of the lower overall fluorine content. Hence, the optimal crosslinker content is found to be

between 30% and 60% DVB depending on the application needed. In what follows, we will favor having high water contact angles and we will use 30% composition as our reference.

Since iCVD coatings can be applied on a wide variety of substrates, we test and compare different polymer performance on poly ethylene terephthalate polyester (PET) fabrics (20 denier warp x 20 denier fill, taken as a reference since, together with nylon, they represent the two main outdoor fabric materials[32]). We observe in **Figure 3c** and **Movie 2** that without treatment, the hydrophilic nature of PET results in immediate water penetration. When coated with a DVB homopolymer (more hydrophobic than PET, see **Figure S2a**), water will bead up if deposited gently but will still soak if impacted. Only the H_1F_7Ma-co-DVB coating will ensure extended water resistance. To understand these behaviors, we rely on the structural nature of most textiles created by weaving yarns made of interlocked fibers (see **Figure 3d**) in a great variety of different patterns (see **Figure 4d**). By modeling their cross section as cylinders piled up in planes (typically going from 3 to 10 layers, see sketch in **Figure 3d**) we assume that the condition for water penetration across the textile (different from imbibition along the fibers[33,34]) is for the contact line at a given layer of cylinders to reach the apex of the layer underneath it. In this framework, if the equilibrium contact angle is low (below 43 degrees[35]) the water will spontaneously wick the medium, as seen for nylon and PET. Between 43 and 90 degrees, even if the substrate is hydrophilic, water will not wick spontaneously but small pressure perturbations or texture defects will allow the water to wick from one level to the next, as seen for the pure DVB coatings. Finally, in the hydrophobic case, considering that contact line has to overcome the advancing contact angle in order to infiltrate a layer of fibers, greater contact angles result in increased water repellency. Since H_1F_7Ma-co-DVB coating is very close to the theoretical limit of 120°, it emerges as an optimal solution. Besides this static performance, H_1F_7Ma-co-DVB also demonstrates suitable dynamic behavior. Indeed, if we look at a side view of a drop impacting on the different fabrics, only the H_1F_7Ma-co-DVB coating (third row in **Figure 4a**) allows the droplet to recoil and roll away after impact. In the other cases (untreated or 100% DVB fabrics) droplets remain attached to the fabric. As a consequence, a liquid layer can build on top of the fabric, decreasing its breathability and locally increasing the water vapor content that facilitates condensation within the structure. To further reduce droplet adhesion, we propose to mechanically roughen the outermost layer of the fabric by micro-sandblasting it and applying the coating onto the structured fabric. This process (described in SI) was chosen because it presents several main advantages: avoiding damage of the overall mechanical properties of the fabric (as would result from chemical[36] etching), being fast, simple and inexpensive (as compared to plasma etching[37]) and achieving more durable treatments (as compared to approaches based on deposition of micro- and nano-feature [38]). We observe in **Figure 4b** the efficient creation of a micrometric high aspect ratio texture by sandblasting a PET fabric for 10 seconds with 10-micron size particles. As a result, impacting droplets can now completely bounce of the surface (**Figure 4b** bottom panel) instead of only being able to roll off (as observed without micro-texture, **Figure 4a** bottom panel).

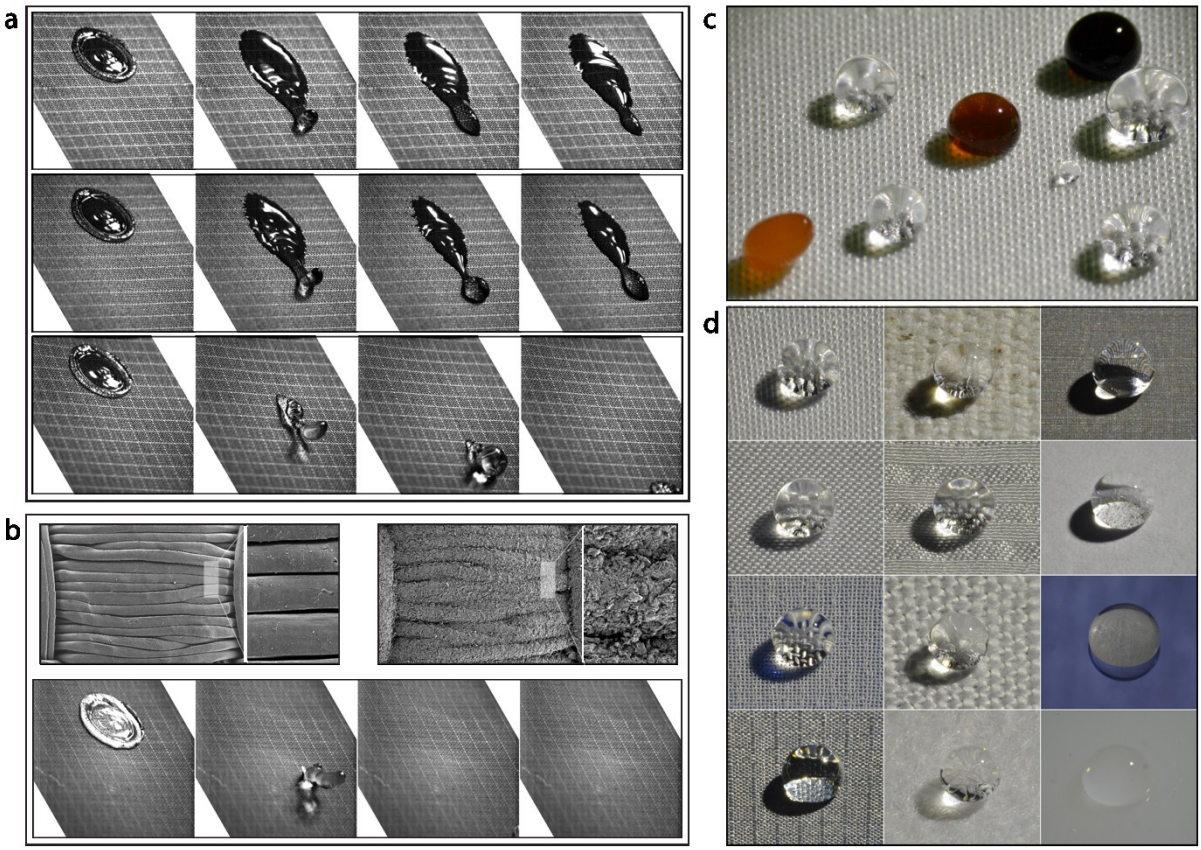

Figure 4. a) Chronophotography of a millimetric water droplet impacting on a 45-degree inclined substrate: bare polyester fabric (top), DVB homopolymer coated fabric (middle) and H_1F_7Ma-co-DVB coated fabric (bottom). Time between frames is 1 ms. Top and middle cases show droplet adhesion after impact and subsequent absorption by the fabric. Only H_1F_7Ma-co-DVB case shows roll off behavior and water resistance. b) Top row: SEM top view of a fabric before (left) and after (right) sand blasting with Al_2O_3 particles of grit #600. Main image and inset view correspond to a x500 and x1000 magnification factor respectively. Bottom row: Chronophotograph of drop impacting on H_1F_7Ma-co-DVB sandblasted fabric, using same conditions as in a). c) Repellency of different liquids on polyester fabric (duchesse luxury satin weave) coated with H_1F_7Ma-co-DVB: soy sauce (black drop), coffee (brown drop), ketchup sauce (orange, non-spherical drop), HCl acid (top left transparent drop), NaOH (bottom right transparent drop) and water (remaining transparent drops). d) Water deposited on different types of H_1F_7Ma-co-DVB coated fabrics. From top to bottom, first column shows different polyester weaves: duchesse satin, duchesse luxury satin, georgette and plain weave. Second column shows different organic materials: cotton, silk, linen and wool. See Movie 3 for a comparison of coated vs non-coated cotton fabric. Third column shows wide range of possible other substrates: silicon nanograss, paper, silicon wafer and nylon.

To show the versatility and performance of the iCVD technique we probe it well beyond the application of water impacting on textiles (**Movie 2**). Indeed, from an everyday application's viewpoint, the durability of the non-wetting fabric is a critical issue. Physical damages can likely occur from abrasions, such as the one originated by the encountering between fabrics. To characterize this type of mechanical durability a laundering test consisting of 10 cold wash machine cycles was performed and no apparent wetting behavior modification was observed (see **Figure 5b**). In addition, abrasion tests (ISO 12947) were performed by abrading the fabric with an increasing number of strokes. **Figure 5a** shows how the wetting behavior of a 20 µL water droplet remains unchanged when deposited onto an iCVD coated fabric abraded up to 10000 times, confirming its durability (above 10000 strokes, fiber damage and breakage became apparent).

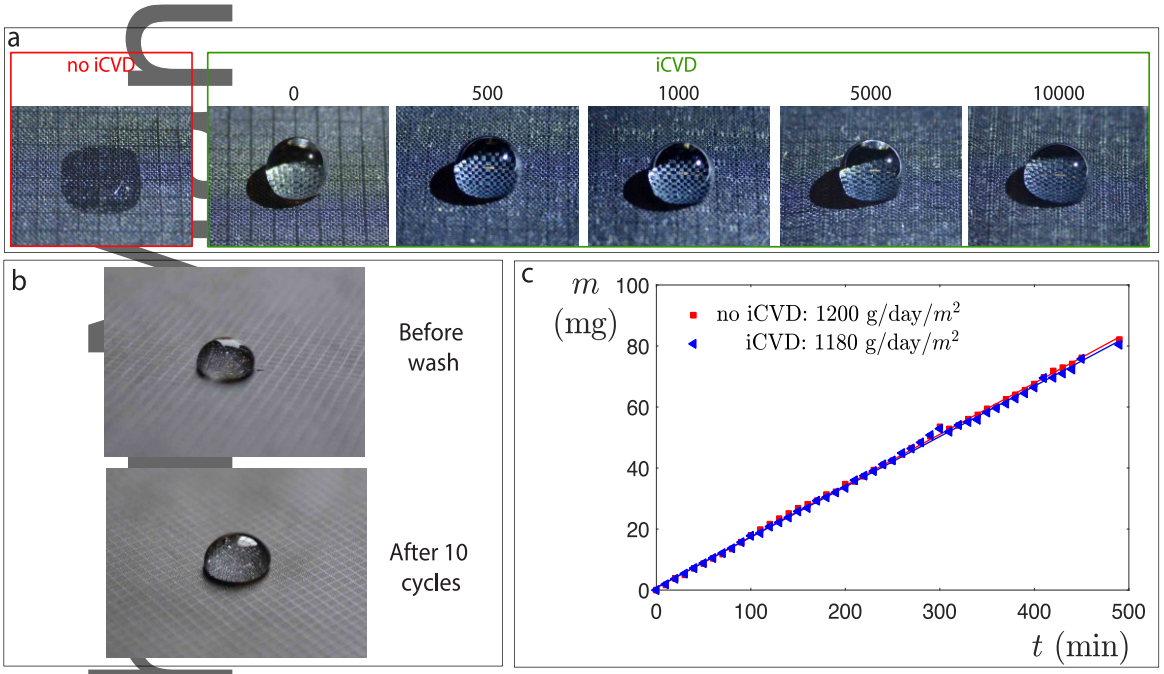

Figure 5: a) Abrasion test comparison. In red, a PET fabric (no iCVD, no abrasion) shows complete absorption of an initial water drop. In green, iCVD coated fabrics exposed to increasing number of abrading strokes: from 0 to 10000 from left to right. Pictures are taken 5 minutes after initial deposition of a 20 µL water drop. b) Water drop deposited on an iCVD coated fabric before (top) and after (bottom) 10 washing cycles. c) Evaporative mass loss as a function of time for iCVD-coated (blue) and non-coated (red) PET fabric. a, b, c) All iCVD coatings are H_1F_7Ma-co-DVB (30% DVB content).

We can also observe in **Figure 4c** very good performance and chemical durability for a wide variety of liquids. Since we did not see any modification of the coated textiles after soaking them for 24 hours in harsh acids or bases (HCl 37% and NaOH 50%), this coating can also be considered to protect surfaces from chemical exposure. In addition, since iCVD allows for ultra-thin conformal coating, initial breathability of the fabric can be maintained. Indeed, **Figure 5c** shows how the initial breathability (1200 ± 20 g/day/m^2) of a non-coated fabric remains almost unchanged after iCVD deposition (1180 ± 20 g/day/m^2). The small difference (1.7 % lower breathability after deposition) is in very good agreement with the 1% thickness change and emphasizes the importance of being able to deposit ultrathin coatings. Regarding low surface tension oils (see SI) we are able to observe much slower impregnation dynamics than compared with the bare fabrics. In order to address a wider variety of substrates, we successfully coated fabrics with different weaves (duchesse, luxury duchesse, georgette, and plain), different materials (cotton, silk, linen and wool) and even more general substrates such as flat nylon, silicon wafer, paper, and nano-textured surfaces (all showing super hydrophobic behavior, see **Figure 4d**).

In summary, our approach allows: 1- to tackle the EPA challenge while exploiting all advantages associated to a vapor deposition technique and 2- to extend the range of application from textiles to any type of substrates and surface coatings. Indeed, the iCVD approach has shown promise as a high-performance coating in the face of regulations banning of longer chain fluorinated polymers. The conformal, ultra-thin, grafted and multi-functionalization aspect of iCVD leads to breathable, low material usage, durable and EPA acceptable coatings. H_1F_7Ma-co-DVB achieves an optimal balance between: surface energy, permitted carbon chain length, and polymer chain rigidity, three parameters critical in the creation of non-wetting fabrics. Additionally, a method for roughening fabrics and creating additional texture has been proposed and shown to improve the performance of the H_1F_7Ma-co-DVB coating. This combined approach has yielded fabrics that repel water impacting from height, as well as oils, acids and bases even after abrasion or laundering aging. Beyond textiles, the iCVD deposition has shown applicability to a variety of substrates ranging from paper to plastics. As a consequence, this work opens the door to new solutions in the coating landscape and paves the way for development of high repellency coatings with large volume production, application of roll-to-roll coating techniques, and multi-functionalization of fabrics and wearable devices.

Experimental Section

iCVD process: all iCVD depositions were conducted in a custom-built reactor previously described.[14,15] Tert-butyl peroxide (TBPO, 97%) initiator was introduced at room temperature into the chamber through a mass flow controller. It underwent activation by hot filament wires placed 2 cm above the samples. The specimen temperature was controlled via a back-cooling recirculation

water system. Monomers were heated to 60 °C for DVB (80%) and 80 °C for H_1F_7Ma (25G) and their flow rates were controlled using needle valves. The chamber pressure was maintained constant during the whole process using a throttle valve. Polymerization thickness was monitored in situ with laser interferometry through the transparent quartz top cover and growth was interrupted when a thickness around 100 nm was attained (typically 10 minutes) ensuring initial color remained unchanged after deposition. The overall composition of each compound was estimated by evaluating their partial pressure and deducting the corresponding fractional saturation percentage. See SI for a more detailed description.

Polymer coating characterization: For each deposition, a flat silicon wafer was placed into the chamber to allow post-polymerization characterization. Film thickness was confirmed through variable-angle ellipsometric spectroscopy (VASE, M-2000, J. A. Woollam), in good agreement with the in-situ laser interferometric measurement. All VASE thickness measurements were performed at 60°, 70° and 80° incidence angle using 190 wavelengths from 315 to 718 nm. A nonlinear least-squares minimization was used to fit ellipsometric data of the films to the Cauchy-Urbach model. The thickness was obtained upon convergence of the algorithm. Fourier transform infrared (FTIR) was performed on a Nicolet Nexus 870 ESP spectrometer equipped with a mercury cadmium tellurium (MCT) detector and KBr beam splitter in normal transmission mode. For the liquid H_1F_7Ma monomer, a DTGS detector was used in combination with a liquid transmission cell (Pike, 6 μm path length). Spectra over 350−3500 cm^{-1} with a resolution of 4 cm^{-1} were collected and averaged over 256 scans to improve signal-to-noise ratio. All spectra were baseline-corrected. Differential Scanning Calorimetry (Discovery DSC, TA instruments) was used to measure the glass transition of H_1F_7Ma homopolymer by ramping up from -90 °C to 120 °C by 2.5°C/min after initial and final temperature equilibration for 5 minutes.

Test: *Laundering* test was performed in a top load washing machine and drying was allowed in between each cold wash cycle. *Abrasion* test ISO 12947 was performed by SDL Atlas on a M235 Martindale abrasion tester with 9kPA pressure weight and 500, 1000, 5000 10000 cycles on PET and cotton iCVD coated fabrics. A Lisajoux pattern and a 100% standard wool abradant where used.

Breathability test (ISO 2528 A-2) was performed by measuring the evaporative mass loss through the cylindrical top open section (16 mm diameter) of a container (20 ml 27x57 glass vial) filled with 16 ml water covered with a PET iCVD coated fabric using a microbalance (Mettler Toledo MS). Data was recorded for 500 minutes in a room at 21 °C and results were compared (see SI) to the case of an untreated fabric.

Supporting Information

Supporting Information is available from the Wiley Online Library or from the author.

Acknowledgements

The authors gratefully acknowledge funding support from Deshpande center at MIT. D.S acknowledges funding support from Translational Fellowship Program at MIT. We thank A. Liu, A. Servi and Y. Jiang for interesting discussions as well as B. Solomon H.L. Girard and P. Moni for help with DSC, AFM and FTIR measurements respectively. This work made use of the Institute for Soldier Nanotechnologies (ISN) at MIT. We thank M. Jansen from SDL Atlas for performing abrasion tests and T. O'Hara for providing fabrics samples.

References

[1] X. Deng, L. Mammen, H.-J. Butt, D. Vollmer, *Science* **2012**, *335*, 67.

[2] M. Liu, S. Wang, L. Jiang, *Nat. Rev. Mater.* **2017**, *2*.

[3] Y. Li, S. Chen, M. Wu, J. Sun, *Adv. Mater.* **2014**, *26*, 3344.

[4] A. Tuteja, W. Choi, M. Ma, J. M. Mabry, S. A. Mazzella, G. C. Rutledge, G. H. McKinley, R. E. Cohen, *Science* **2007**, *318*, 1618.

[5] S. T. Iacono, S. M. Budy, D. W. Smith, J. M. Mabry, *J. Mater. Chem.* **2010**, *20*, 2979.

[6] A. C. Glavan, R. V. Martinez, A. B. Subramaniam, H. J. Yoon, R. M. D. Nunes, H. Lange, M. M. Thuo, G. M. Whitesides, *Adv. Funct. Mater.* **2014**, *24*, 60.

[7] OECD/UNEP Global PFC Group, *Environ. Health Saf. Environ. Dir. OECD* **2013**.

[8] Environmental Protection Agency, *US Environ. Prot. Agency* **2009**, *12*, 30.

[9] G. Akovali, *Advances in Polymer Coated Textiles*, Smithers Rapra, **2012**.

[10] A. M. Coclite, R. M. Howden, D. C. Borrelli, C. D. Petruczok, R. Yang, J. L. Yagüe, A. Ugur, N. Chen, S. Lee, W. J. Jo, A. Liu, X. Wang, K. K. Gleason, *Adv. Mater.* **2013**, *25*, 5392.

[11] A. Ugur, F. Katmis, M. Li, L. Wu, Y. Zhu, K. K. Varanasi, K. K. Gleason, *Adv. Mater.* **2015**, *27*, 4604.

[12] L. C. Bradley, M. Gupta, *Langmuir* **2015**, *31*, 7999.

[13] H. S. Suh, D. H. Kim, P. Moni, S. Xiong, L. E. Ocola, N. J. Zaluzec, K. K. Gleason, P. F. Nealey, *Nat. Nanotechnol.* **2017**.

[14] A. T. Paxson, J. L. Yagüe, K. K. Gleason, K. K. Varanasi, *Adv. Mater.* **2014**, *26*, 418.

[15] A. Liu, E. Goktekin, K. K. Gleason, *Langmuir* **2014**, *30*, 14189.

[16] Q. Zhang, Q. Wang, J. Jiang, X. Zhan, F. Chen, *Langmuir* **2015**, *31*, 4752.

[17] J. Williams, *Waterproof and Water Repellent Textiles and Clothing - 1st Edition*, Woodhead Publishing, **2017**.

[18] J. A. Kleingartner, H. Lee, M. F. Rubner, G. H. McKinley, R. E. Cohen, *Soft Matter* **2013**, *9*, 6080.

[19] M. Beiner, H. Huth, *Nat. Mater.* **2003**, *2*, 595.

[20] K. A. O'Leary, D. R. Paul, *Polymer* **2006**, *47*, 1245.

[21] Y. Yoo, J. B. You, W. Choi, S. G. Im, *Polym. Chem.* **2013**, *4*, 1664.

[22] A. M. Coclite, Y. Shi, K. K. Gleason, *Adv. Mater.* **2012**, *24*, 4534.

[23] Q. Zhang, Q. Wang, X. Zhan, F. Chen, *Ind. Eng. Chem. Res.* **2014**, *53*, 8026.

[24] K. Honda, I. Yamamoto, M. Morita, H. Yamaguchi, H. Arita, R. Ishige, Y. Higaki, A. Takahara, *Polymer* **2014**, *55*, 6303.

[25] Q. Wang, Q. Zhang, X. Zhan, F. Chen, *J. Polym. Sci. Part Polym. Chem.* **2010**, *48*, 2584.

[26] F. Fleischhaker, A. P. Haehnel, A. M. Misske, M. Blanchot, S. Haremza, C. Barner-Kowollik, *Macromol. Chem. Phys.* **2014**, *215*, 1192.

[27] T. Hirabayashi, T. Kikuta, K. Kasabou, K. Yokota, *Polym. J.* **1988**, *20*, 693.

[28] G. G. Odian, *Principles of Polymerization*, Wiley-Interscience, Hoboken, N.J, Ch.3, **2004**.

[29] R. Mukherjee, A. Sharma, *Soft Matter* **2015**, *11*, 8717.

[30] V. Starov, I. Ivanov, Eds. , *Fluid Mechanics of Surfactant and Polymer Solutions*, Springer Vienna, Vienna, **2004**.

[31] R. W. Style, E. R. Dufresne, *Soft Matter* **2012**, *8*, 7177.

[32] R. R. Mather, R. H. Wardman, *The Chemistry of Textile Fibers*, Royal Society Of Chemistry, Cambridge, **2010**.

[33] I. Pezron, G. Bourgain, D. Quéré, *J. Colloid Interface Sci.* **1995**, *173*, 319.

[34] C. Duprat, S. Protière, A. Y. Beebe, H. A. Stone, *Nature* **2012**, *482*, 510.

[35] P. S. Raux, H. Cockenpot, M. Ramaioli, D. Quéré, C. Clanet, *Langmuir* **2013**, *29*, 3636.

[36] C.-H. Xue, X.-J. Guo, M.-M. Zhang, J.-Z. Ma, S.-T. Jia, *J. Mater. Chem. A* **2015**, *3*, 21797.

[37] B. Shin, K.-R. Lee, M.-W. Moon, H.-Y. Kim, *Soft Matter* **2012**, *8*, 1817.

[38] J. A. Kleingartner, S. Srinivasan, Q. T. Truong, M. Sieber, R. E. Cohen, G. H. McKinley, *Langmuir* **2015**.

TOC:

iCVD deposition of conformal short fluorinated polymers stabilized with a crosslinking agent is successfully carried out with 1*H*,1*H*-Perfluorooctyl methacrylate crosslinked with divinylbenzene. The ultra-thin, grafted and multi-functionalization aspect of iCVD leads to breathable, low material usage, durable and EPA acceptable liquid repellent coatings particularly suited for substrates as diverse as fabrics, paper, and nano-textured silicon.